Reduction of Alkyl Halides by Homonuclear Bridging Hydride, $(\mu\text{-H})[(\eta^5\text{-MeCp})Mn(CO)_2]_2^-PPN^+$ [1)]

Yong Kwang Park* and Young Woong Kim

Department of Chemistry, Kangwon National University, Chuncheon 200-701, Korea

Received November 15, 1995

Alkyl halides were reduced to the corresponding alkanes by the homonuclear bridging hydride, $(\mu\text{-H})[(\eta^5\text{-MeCp})Mn(CO)_2]_2^-PPN^+$ in THF at the elevated temperatures (40°-60 °C) under the pseudo first order reaction conditions where excess of alkyl halide was employed under nitrogen atmosphere. The reaction is of overall second order; first order with respect to [bridging hydride] and first order with respect to [alkyl halide] with the activation parameters, $\Delta H^{\neq}=28.93$ kcal/mol and $\Delta S^{\neq}=17.95$ e.u. The kinetic data, the ESR evidence and the reaction with cyclopropyl canbinyl bromide ensure that two possible reaction pathways are operable in this reaction: (1) concerted mechanism, and (2) single electron transfer pathway are in competition leading to the same product, the corresponding alkane.

Introduction

The hydride/halide exchange is observed in the reaction of anionic transition metal hydride with organic halide. An extensive mechanistic studies on $HM(CO)_4L^-$ (M=Cr, W; L=CO, PR_3) have been performed in connection with organic halides.[1] However, almost no mechanistic investigation has been recently made as to the reaction of anionic transition metal bridging hydride with organic halide probably due to the inherent difficulty of preparing the bridging hydride complex and its lower reactivity relative to the usual anionic terminal hydride complex. It is, of course, generally believed that bridging hydride usually have another metal moiety which may play a Lewis acid role in connection with the corresponding terminal hydride; therefore, it should definitely sacrifice its reactivity. On reacting with organic halide as a hydride transfer agent, it should fall apart into two metal moieties,[2] which may render the mechanistic investigation even more difficult. Here we report kinetic investigations on the reaction of $(\mu\text{-H})[(\eta^5\text{-MeCp})Mn(CO)_2]_2(PPN)$ with alkyl halides in THF under the pseudo first order conditions.

Experimental

An inert-atmosphere glove box, Schlenk wares and high vacuum line were employed for most of sample transfers and manipulations. Infrared spectra were recorded on a Perkin-Elmer 238B spectrophotometer using 0.10 mm sealed CaF_2, KBr or NaCl solution cells. ^1H NMR spectra were recorded on a Varian Gemini-200 spectrometer. ESR spectra were obtained from a Bruker ER-200D spectrometer. Reaction temperatures were maintained with a Haake A 81 thermostat. Elemental analyses were conducted at the Organic reaction center, Sogang University.

Photoreactions were performed using a 550 watt Hg vapor lamp covering a rather broad range of UV-VIS wavelengths. Solvents were distilled and degassed under N_2 atmosphere from appropriate drying and O_2 scavenging agents. All other liquid substrates were degassed by the freeze-pump-thaw cycles before being used in the drybox or under Ar. All other reagents were purchased from ordinary vendors and used as received without further purification.

Preparation of $(\eta^5\text{-MeCp})Mn(CO)_2(THF)$. The preparation procedure of $(\eta^5\text{-MeCp})Mn(CO)_2(THF)$ is similar to a method in the literature.[3] A solution of tricarbonyl(η^5-methylcyclopentadienyl)manganese (I) (0.654 g, 3.0 mmol) in freshly distilled THF (90 mL) is photolyzed for 24 min. with a nitrogen purge, or until >80% of the IR bands of the tricarbonyl complex (ν(CO); 2010(s), 1924(s) cm^{-1}) is replaced by those of $(\eta^5\text{-MeCp})Mn(CO)_2(THF)$ (ν(CO); 1917(s), 1840(s) cm^{-1}). A slow, steady flow of N_2 through the solution during photolysis assists in removal of CO and prevents reversible back-reaction. Because of the toxicity of the CO evolved, all the reactions should be run in a well-ventilated fume hood.

Preparation of $(\eta^5\text{-MeCp})Mn(CO)_2(pip)$. A solution of tricarbonyl(η^5-methylcyclopentadienyl)manganese (I) (1.162 g, 5.03 mmol) and piperidine (1 mL, 2 equivalents) in freshly distilled THF (90 mL) is photolyzed for 30 min with a nitrogen purge, or until the IR bands of the tricarbonyl complex (ν(CO); 2010(s), 1924(s) cm^{-1}) are replaced by those of $(\eta^5\text{-MeCp})Mn(CO)_2(pip)$ (ν(CO); 1902(s), 1830(s) cm^{-1}). After the photolysis, the solution was concentrated to about 1/4 of its initial volume under vacuum and hexane was added slowly until a orange precipitate was formed on the bottom. And then 50 mL of hexane was added and the solution was removed by cannula. The product was dried under vacuum. The yield was 1.45 g (78%). This product is very stable in the glovebox and stable in air for a short period of time.

Preparation of $(\mu\text{-H})[(\eta^5\text{-MeCp})Mn(CO)_2]_2^-PPN^+$. THF solution (90 mL) of $(\eta^5\text{-MeCp})Mn(CO)_2(THF)$ (3.0 mmol) freshly prepared from the photolysis was added to the ethanol solution (10 mL) of $PPNBH_4$[4] (0.55 g, 1.0 mmol). The mixed solution was stirred for more than one hour at ambient temperature. The solution was concentrated and then ether (or hexane) was added slowly until a dark green precipitate was formed on the bottom. The upper part of the solution was removed by a cannula and the residual solvent was removed in vacuo. And then THF (40 mL) was added and the mother liquor was passed through a Celite column to remove unreacted $PPNBH_4$ and transferred *via* cannula to another Schlenk flask. The solution was concentrated to

[1)] PPN^+ = bis(triphenylphosphine)iminium cation

about 1/4 of its initial volume under vacuum and ether was added slowly until a dark green precipitate was formed on the bottom. The product dried under vacuum weighed 0.65 g (71% yield). The product was stable for about 3 days in THF and for almost a month under N_2 at ambient temperature. Anal. Calcd. for $C_{52}H_{45}Mn_2NO_4P_2$: C, 67.99; H, 4.94; N, 1.53 Found: C, 67.80; H, 4.78; N, 1.50. ν(CO) IR (THF) in cm^{-1}; 1890(w), 1864(s), 1815(s). ^1H NMR (DMSO-d_6) in δ (ppm); −26.8 (s, μ-H), 1.91 (s, $2CH_3$), 3.40 (d, $2CH_2$), 4.12 (d, $2CH_2$), 7.64-7.79 (m, $6C_6H_5$).

General Procedure for the Reaction of (μ-H)[(η⁵-MeCp)Mn(CO)₂]₂⁻PPN⁺ with RX. Usually 10 mL of THF was added to the mixture of (μ-H)[(η⁵-MeCp)Mn(CO)₂]₂⁻PPN⁺ (0.046 g, 0.05 mmol) and an excess of RX in a 10 mL vol. flask *via* syringe under nitrogen at ambient temperature. The solution was shaken for a few minutes prior to being kept in a water bath set at a specific temperature close to the boiling point of the RX due to the mild reactivity of the bridging metal hydride. Rates of the reaction were observed by the decrease in absorbance of the intense isolated CO stretching band (1864 cm^{-1}) of the reactant, which does not overlap with those of products. Products, (η⁵-MeCp)Mn(CO)₃ and (η⁵-MeCp)Mn(CO)₂X⁻PPN⁺, were identified by their ν(CO) IR spectra as compared with previously isolated compounds characterized in our laboratory.

ESR Study of the Reaction of (η⁵-MeCp)Mn(CO)₂(H)⁻PPN⁺ with RX. After the methanolic protonation of (η⁵-MeCp)Mn(CO)₂(pip), the solution was transferred to a vessel on which the DMPO (5,5-dimethyl-1-pyrroline-N-oxide) was loaded and an alkyl halide was added in situ. After mixing with alkyl halide, the paramagnetic product was identified by ESR. (Figure 5)

Kinetic Measurements. Inside the glovebox, solid samples (0.05 mmol) of hydrides were placed in a vial (15 mL capacity) with a small septum cap tightly wired to its outlet. Outside the box, an appropriate solvent (10 mL) was added, and the flask was immersed in a constant temperature bath. After the temperature was equilibrated (*ca.* 5 min), of an organic halide solution pre-equilibrated to the same temperature was introduced and timing began. Except where noted, the organic halide concentrations were in quite excess with regard to the hydride, ensuring pseudo-first-order reaction conditions. Samples (*ca.* 0.1 mL) were periodically withdrawn, and the reaction rate was monitored by the decrease in intensity of an isolated ν(CO) infrared absorbance of the hydride. Rate constants were calculated by using a linear least-squares program for the pseudo-first-order rate plots of ln (A_t-A_∞) *vs.* time, where A_t is the absorbance at time t and A_∞ is the absorbance at time infinity. The observed rate constants (k_{obs}), the standard deviation, and the error at the chosen confidence limit were calculated by using standard least-squares fitting programs. Second-order rate constants (k_2) were obtained by dividing k_{obs} by [RX]. Activation parameters ($\Delta H^{\ddagger}$ and $\Delta S^{\ddagger}$) were obtained by plotting -lnk_2 *vs.* 1/T, where T is the temperature (K) of each individual run. Again, a standard computer program was used for the data processing and the error analysis at the chosen confidence level.

Results and Discussion

Table 1. IR spectral data for the various complexes

Complexes	Medium	ν(CO), cm^{-1}
(η⁵-MeCp)Mn(CO)₃	THF	2010(s), 1924(s)
(η⁵-MeCp)Mn(CO)₂(THF)	THF	1917(s), 1840(s)
(η⁵-MeCp)Mn(CO)₂(pip)	THF	1902(s), 1830(s)
(η⁵-MeCp)Mn(CO)₂(H)⁻PPN⁺	THF	1890(s), 1815(s)
(η⁵-MeCp)Mn(CO)₂(H)⁻Na⁺	THF	1924(s), 1858(s), 1828(w)
(μ-H)[(η⁵-MeCp)Mn(CO)₂]₂⁻PPN⁺	THF	1890(w), 1864(s), 1815(s)
(η⁵-MeCp)Mn(CO)₂Cl⁻PPN⁺	THF	1893(s), 1816(s)
(η⁵-MeCp)Mn(CO)₂Br⁻PPN⁺	THF	1892(s), 1817(s)
(η⁵-MeCp)Mn(CO)₂I⁻PPN⁺	THF	1892(s), 1820(s)

Reactions of (μ-H)[(η⁵-MeCp)Mn(CO)₂]₂(PPN) with Alkyl Halides. Reactions of (μ-H)[(η⁵-MeCp)Mn(CO)₂]₂(PPN) (0.046 g; 0.05 mmol) with an excess of alkyl halides were usually performed in THF at the specific temperature close to the boiling point of the corresponding alkyl halides. Alkanes as products were characterized by GC-MASS and (η⁵-MeCp)Mn(CO)₂X⁻PPN⁺ (X=I, Br, Cl) could be identified by the respective ν(CO) IR spectra as compared with those of the previously reported compounds in our laboratory.[5] However, in addition to the above two products, (η⁵-MeCp)Mn(CO)₃ was also obtained presumably due to the reaction of CO from the (η⁵-MeCp)Mn(CO)₂ decomposition in THF with another (η⁵-MeCp)Mn(CO)₂ moiety on removal of hydride by alkyl halide. (η⁵-MeCp)Mn(CO)₃ on UV irradiation in THF was also observed to form (η⁵-MeCp)Mn(CO)₂(THF) adduct (ν(CO) IR; 1917(s), 1840(s) cm^{-1}) under nitrogen atmosphere at ambient temperature; however, on prolonged time (a few hours) it gradually decomposed to yield stable (η⁵-MeCp)Mn(CO)₃ probably due to the reaction (η⁵-MnCp)Mn(CO)₂(THF) with the dissolved CO.

$$(\mu\text{-H})[(\eta^5\text{-MeCp})\text{Mn(CO)}_2]_2(\text{PPN}) + \text{R-X} \rightarrow (\eta^5\text{-MeCp})\text{Mn(CO)}_3(\text{major}) + \text{R-H} + (\eta^5\text{-MeCp})\text{Mn(CO)}_2\text{X}^-\text{PPN}^+(\text{minor}) + \text{PPN}^+\text{X}^-$$

Electronic phenomena on (η⁵-MeCp)Mn(CO)₂X (X =H⁻, CO, THF, Cl⁻, Br⁻, I⁻) in THF. Table 1 shows ν(CO) IR for (η⁵-MeCp)Mn(CO)₂X(X=H⁻, CO, THF, Cl⁻, Br⁻, I⁻) in THF. Based on the positions of ν(CO) IR, the following trend is found in the order of donating electron density of the ligands to the metal center (Mn) of (η⁵-MeCp)Mn(CO)₂X.

$$H^- \sim Cl^- \sim Br^- \sim I^- > \text{peperidine} > \text{THF} > CO$$

However, it is worthwhile to note that in Na⁺(η⁵-MeCp)Mn(CO)₂H⁻, Na⁺ seems to interact with H⁻ of this Mn hydride so that the electron density on Mn may be somewhat less than that of PPN⁺(η⁵-MeCp)Mn(CO)₂H⁻; therefore, H⁻ of Na⁺ salt has obviously much more electron density than that of PPN⁺ salt, as is evidenced by the higher ν(CO) IR of the Na⁺(η⁵-MeCp)Mn(CO)₂H⁻ than that of PPN⁺ analogue (1890, 1815 cm^{-1} for PPN⁺Mn hydride; 1924, 1858, for Na⁺ one).

The weak band at 1828 cm^{-1} may be ascribed to Na⁺

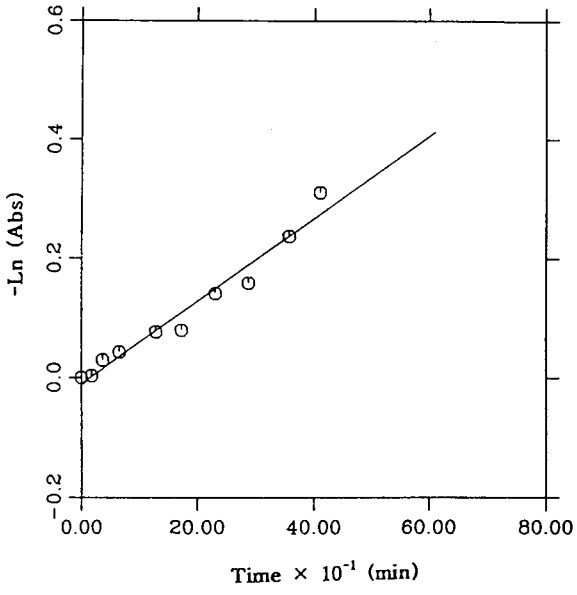

Figure 1. Pseudo-first-order plot of the reaction of (μ-H)[(η⁵-MeCp)Mn(CO)₂]₂⁻PPN⁺ (5.0 mM) with CH_3CH_2I (50.0 mM) in THF at 40.0 ℃.

Table 2. The relationship between CH_3CH_2I concentrations and the rates k_{obs} for the reaction of (μ-H)[(η⁵-MeCp)Mn(CO)₂]₂⁻PPN⁺ in THF at 60 ℃

[Metal Hydride] M (×10³)	[CH_3CH_2I] M (×10³) (fold)	$k_{obs}\times10^4$ s^{-1}
5.0	50.0 (10)	2.97± 0.19
5.0	100 (20)	4.62± 0.40
5.0	150 (30)	8.67± 1.00
5.0	200 (40)	11.4± 1.11

interaction with the coordinated CO of the manganese hydride.[6] As there is less electron density on Mn of the terminal hydride, the reactivity of the bridging hydride is assumed to be lower than that of the terminal hydride; however, the bridging hydride seems to be much more thermally stable probably due to the possible delocalization of the electron density on manganese through another (η⁵-MeCp)Mn moiety.

Determination of Activation Parameters. The reaction of the bridging manganese hydride with alkyl halide usually proceeds at a rate convenient for monitoring by conventional ν(CO) IR technique. Reactions of the bridging hydride with alkyl halide were carried out under the pseudo first order conditions where an excess alkyl halide was used (Figure 1 and Table 2). For the reaction of the bridging manganese hydride with ethyl iodide, an overall second order kinetics was established; first order with respect to [bridging manganese hydride] and another first order with respect to [ethyl iodide] (Table 2).

The ethyl iodide concentrations were varied from 10- to a 50-fold excess with regard to the manganese hydride one. Table 2 shows that the rate is linearly dependent upon the ethyl iodide concentration. This reaction seems to be accelerated by the increase in the reaction temperature, which is evidenced by Table 3. Figure 2 also shows a good linearity between the rate and ethyl iodide concentration.

Table 3. Temperature dependence on the reaction of (μ-H)[(η⁵-MeCp)Mn(CO)₂]₂⁻PPN⁺ with CH_3CH_2I in THF

[Metal Hydride] M (×10³)	[CH_3CH_2I] M (×10³) (fold)	Temp. (℃)	$k_{obs}\times10^4$ s^{-1}
5.0	100(20)	40	0.41± 0.02
5.0	100(20)	50	1.92± 0.20
5.0	100(20)	60	4.62± 0.40

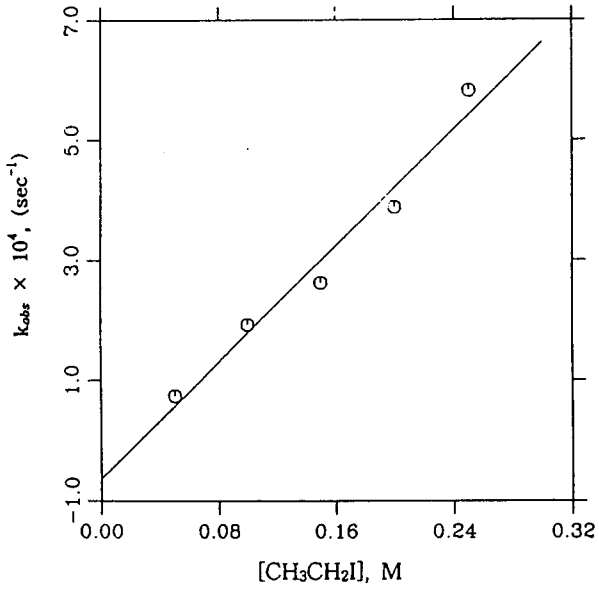

Figure 2. Plot for k_{obs} *vs* [CH_3CH_2I] for the reaction of (μ-H)[(η⁵-MeCp)Mn(CO)₂]₂⁻PPN⁺ in THF at 50.0 ℃.

reaction rate=k_2[bridging manganese hydride][ethyl iodide]

Activation parameters ($\Delta H^{\neq}$=28.93± 2.18 kcal/mol; $\Delta S^{\neq}$= 17.95± 11.20 e.u.) calculated from the Eyring plot (Figure 3) suggest more of dissociative character at the rate-determining step of the reaction even though this reaction shows overall second order kinetics. This rather surprising phenomenon implies that two reactants, the bridging manganese hydride and ethyl iodide, on reaction afford the four products, (η⁵-MeCp)Mn(CO)₃, (η⁵-MeCp)Mn(CO)₂I⁻PPN⁺, PPN⁺I⁻ and ethane.

Mechanistic Considerations. It is quite often observed that hydride (H^-)/halide displacement takes place in the reaction of anionic terminal transition metal hydride with alkyl halide. However, in this reaction involving bridging manganese hydride, (η⁵-MeCp)Mn(CO)₃, ethane, and PPN⁺I⁻ were observed as major products. Figure 4 shows ν(CO)IR spectral variations of reactant (manganese bridging hydride; D, E) and product (MeCpMn(CO)₃; A, B) during the reaction at 45 ℃ in THF with ethyl iodide, where the reactant concentration diminishes gradually and the product concentration increases simultaneously as well; however, at the end of

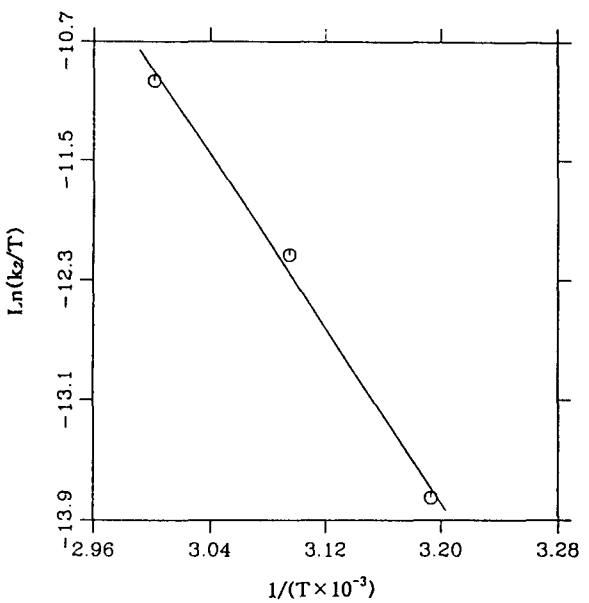

Figure 3. Eyring plot for the reaction $(\mu\text{-H})[(\eta^5\text{-MeCp})Mn(CO)_2]_2^-$ PPN^+ (5.0 mM) with CH_3CH_2I (150 mM) in THF.

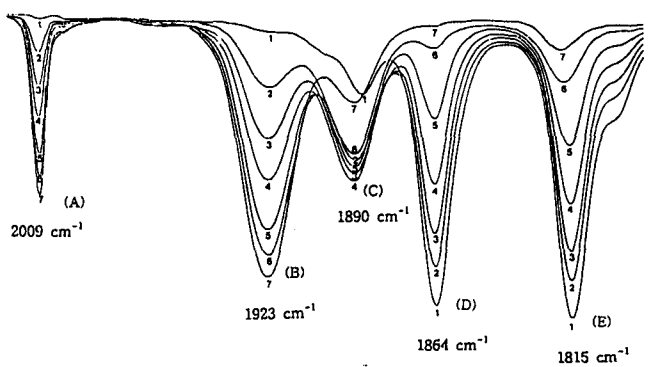

Figure 4. The ν(CO) IR spectral variations during the reaction of $(\mu\text{-H})[(\eta^5\text{-MeCp})Mn(CO)_2]_2^-PPN^+$ with CH_3CH_2I (150 mM) in THF at 45.0 ℃.

the reaction the two bands (C and E) appeared rather in small concentration, which suggests the formation of $MeCpMn(CO)_2I^-$ as a minor product.

The concentration of $MeCpMn(CO)_2I^-PPN^+$ increases gradually at first and then decreases later though, in small amount; however, it never disappears at the end of the reaction, which implies that this species is a product rather than an intermediate, but this thermally unstable species may slowly decompose to PPN^+I^- and $MeCpMn(CO)_3$ on recombination of $MeCpMn(CO)_2$ moiety with either solvent-trapped CO or coordinated CO ligand of another manganese hydride moiety through structural reorganization at the elevated temperatures (40℃-60℃). However, $MeCpMn(CO)_2(THF)$ does not appear as an intermediate during the reaction (Figure 4). Based on the above-mentioned observations together with the kinetic results, the following reaction pathways may be proposed:

A. Consecutive Hydride Transfer

$$(MeCp)(OC)_2Mn\text{-}H\text{-}Mn(CO)_2(CpMe)^- \underset{THF}{\overset{r.d.s.}{\rightleftharpoons}} (MeCp)(OC)_2MnH^- + (MeCp)(OC)_2Mn(THF)$$

$$(MeCp)(OC)_2MnH^- + CH_3CH_2I \xrightarrow[THF]{} (MeCp)(OC)_2Mn(THF) + CH_3CH_3 + I^-$$

$$(MeCp)(OC)_2Mn(THF) + I^- \longrightarrow (MeCp)(OC)_2MnI^- + THF$$

$$(MeCp)(OC)_2Mn(THF) + CO \longrightarrow (MeCp)(OC)_3Mn + THF$$

B. Single Electron Transfer

$$(MeCp)(OC)_2Mn\text{-}H\text{-}Mn(CO)_2(CpMe)^- + CH_3CH_2I \rightarrow 2(MeCp)Mn(CO)_2 + H\cdot + [CH_3CH_2I]^-$$

$$[CH_3CH_2I]^- \rightarrow CH_3CH_2\cdot + I^-$$

$$CH_3CH_2\cdot + \cdot H \rightarrow CH_3CH_3$$

$$(MeCp)Mn(CO)_2 + I^- \rightarrow (MeCp)Mn(CO)_2I^-$$

$$(MeCp)Mn(CO)_2 + CO \rightarrow (MeCp)Mn(CO)_3$$

C. Concerted Pathway (Modified)

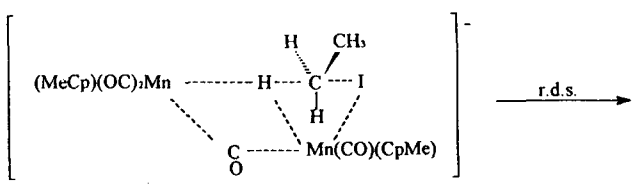

$$(MeCp)(OC)_3Mn + CH_3CH_3 + (MeCp)(OC)MnI^-$$

$$(MeCp)Mn(CO)I^- + CO \rightarrow (MeCp)Mn(CO)_2I^-$$

In case of hydride transfer (mechanism A), this manganese bridging hydride should be divided into manganese terminal hydride, $(MeCp)Mn(CO)_2H^-$ and $(MeCp)Mn(CO)_2$ moiety at the rate-determining step, followed by the reaction of the terminal hydride with ethyl iodide; however, this reaction definitely needs another activation energy barrier similar to the previous rate-determining step. Therefore, this consecutive hydride transfer reaction should have more complicated rate expression than the overall second order kinetics we already observed.

In case the terminal hydride's reaction takes place quite faster than the bridging hydride's one, this overall rate expression should be of first order with respect to the bridging hydride concentration, which is not consistent with the observed kinetics. This terminal hydride can also react with $(MeCp)Mn(CO)_2(THF)$ to go back to the bridging hydride very quickly even at ambient temperature while for another reaction involving ethyl iodide, it seems definitely to happen slowly due to the energy required for bond cleavages (H-Mn and C-I); however, the latter reaction may have some kinetic advantage over the former one becomes ethyl iodide was usually used quite in excess (≥20 times) to the $(MeCp)Mn(CO)_2(THF)$.

Here, $(MeCp)Mn(CO)_2(THF)$ reacts with either CO or I^- as a reactive intermediate; however, no ν(CO) IR represent $(MeCp)Mn(CO)_2(THF)$ (1917, 1840) (Figure 4), which may

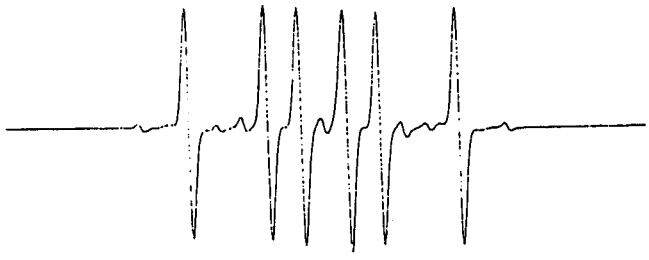

Figure 5. ESR hyperfine splitting pattern for the reaction of $(\mu\text{-H})[(\eta^5\text{-MeCp})Mn(CO)_2]_2$(PPN) with $CH_3CH_2CH_2I$ in THF in the presence of DMPO at ambient temperature under nitrogen.

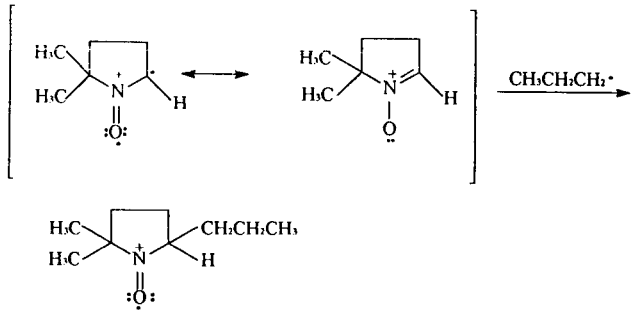

Scl

be another drawback in supporting this reaction pathway.

Secondly, single electron transfer mechanism can be a good candidate for describing this reaction. The overall second kinetics and positive entropy change seems to be consistent with this pathway because on one electron transfer from the manganese bridging hydride to ethyl iodide, the manganese bridging hydride radical may decompose to the three moieties; two $(MeCp)Mn(CO)_2$ and H· readily. However, it may be somewhat surprising to observe $(MeCp)Mn(CO)_3$ as a major product because there would be a definitely limited concentration of CO in THF at the elevated temperature. The $(MeCp)Mn(CO)_2$ moiety, 16 electron species, can never the less react readily with either CO or I^- to yield the corresponding products.

It may not be unreasonable to predict that the manganese bridging hydride radical may pick up I^- from $[CH_3CH_2I]^{\cdot-}$, thereby rendering bridging CO, which causes $(MeCp)Mn(CO)_3$, and $(MeCp)Mn(CO)I^-$ as predicted in the following concerted pathway. If this is the case for single electron transfer pathway, the mechanism may be revised in the following:

$$(MeCp)(OC)_2Mn\text{-}H\text{-}Mn(CO)_2(CpMe) + CH_3CH_2I \rightarrow$$

$$H\cdot + (MeCp)Mn(CO)_3 + (MeCp)Mn(CO)I^- + CH_3CH_2\cdot$$

$$CH_3CH_2\cdot + \cdot H \rightarrow CH_3CH_3$$

$$(MeCp)Mn(CO)I^- + CO \rightarrow (MeCp)Mn(CO)_2I^-$$

In this way we may better describe the formation of $(MeCp)Mn(CO)_3$ and $(MeCp)Mn(CO)_2I^-$ as well. This reaction mechanism is further supported by the ESR experimental data. We observed evidence for propyl radical formation from the reaction of the bridging manganese hydride with

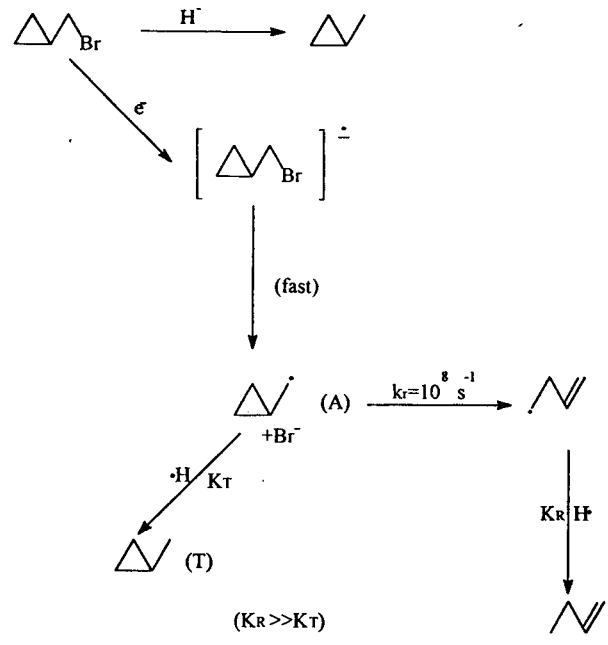

Scheme 2.

propyl iodide in THF at ambient temperature under nitrogen atmosphere in presence of the radical trapping agent, DMPO (5,5-dimethyl-1-pyrroline-N-oxide); the sextet hyperfine splitting pattern represents the more stable corresponding radical (Figure 5 and Scheme 1).

The sextet consists of two groups of triplet arising from one $^{14}N(I=1)$ and $^1H(I=1/2)$ nuclei($a_H=20.02G$; $a_N=14.01G$); these similar values are usually observed where alkyl group is attached to the carbon neighboring nitrogen of this stable radical[7] (Scheme 1).

Of course, no appreciable ESR patterns were observed in the same reaction mixture without the above-mentioned radical trapping agent.

To ensure this single electron transfer, we tried another reaction with cyclopropylcarbinyl bromide; the product distribution of methylcyclopropane and 1-butene (*ca.* 1 : 1.5 by GC peak area) may be another evidence for this pathway (Scheme 2).[8]

However, it is also worthwhile to note that, in this reaction, two pathways (methyl cyclopropane for H^- transfer; 1-butene for SET) are possible. Here, the possible H^- transfer may be related to the following modified concerted mechanism, not the previously described hydride transfer (Scheme 2).

Thirdly, modified concerted mechanism can be thought of as another alternative description for this reaction. This pathway seems to be consistent with the second order kinetics with the positive entropy change of activation.

It also shows the formation of $(MeCp)Mn(CO)_3$ and $(MeCp)Mn(CO)_2I^-$, respectively without much difficulty. In this concerted mechanism, the major criteria for the successful description may lie in the structure of the proposed transition state where H^- should be in close proximity to the carbon attached to iodide and iodide also in the vicinity of manganese metal center; therefore, H^- is transferred to the carbon neighboring iodide and carbonyl ligand migrates from the

manganese which iodide approaches so as to form (MeCp)Mn $(CO)_3$.

Once $(MeCp)Mn(CO)I^-$ is formed, it may readily pick up one CO to have $(MeCp)Mn(CO)_2I^-$, if only the dissolved CO is available. The methyl cyclopropane from the reaction involving cyclopropylcarbinyl bromide may be assumed to support, in part, this concerted mechanism.

In conclusion, the last two reaction pathways, SET and the concerted pathways may operate in competition in this reaction.

Acknowledgment. Financial support from the Korea Science and Engineering Foundation (92-25-00-04) is greatly appreciated. The authors thank Mrs. M. S. Kim and Mr. D. S. Yun for their preparing this manuscript. Fruitful discussions with Professor G. S. Kim is highly appreciated. Authors also thank the referees for their advice and corrections on this manuscript.

References

1. (a) Kao, S. C.; Spillet, C. T.; Ash, C.; Lusk, R.; Park, Y. K.; Darensbourg, M. Y. *Organometallics* **1985**, *4*, 83. (b) Kao, S. C.; Darensbourg, M. Y. *Organometallics* **1984**, *3*, 646.
2. (a) Arndt, L.; Delord, T.; Darensbourg, M. Y. *J. Am. Chem. Soc.* **1984**, *106*, 456. (b) Slater, S. G.; Lusk, R.; Schumann, B.; Darensbourg, M. Y. *Organometallics* **1982**, *1*, 1662.
3. (a) Nyholm, R. S.; Sabdhu, S. S. *J. Chem. Soc.* **1963**, *92*, 5916. (b) Butler, I. S.; Coville, N. J.; Cozak, D. and *et al. Inorg. Synth.* **1978**, *19*, 188. (c) Zhuang, Jun-Ming; Batchelor, R. J.; Einstein, F. W. B.; Jones, R. H.; Hader, R.; Sutton, D. *Organometallics* **1990**, *9*, 2725. (d) Wieland, S.; Eldik, R. V. *Organometallics* **1991**, *10*, 3110.
4. Kirtley, S. W.; Andrews, M. A.; Bau, R.; Grynkewich, G. W.; Marks, T. J.; Tipton, D. L.; Whittlesey, B. R. *J. Am. Chem. Soc.* **1977**, *99*, 7154.
5. Park, Y. K.; Lee, Y. G.; Kim, G. S. *Bull. Korean Chem. Soc.* (submitted in 1995).
6. (a) Darensbourg, M. Y.; Jimenez, P.; Sackett, J. R.; Hankel, J. M.; Kump, R. L. *J. Am. Chem. Soc.* **1982**, *104*, 1521. (b) Darensbourg, M. Y.; Darensbourg, D. J.; Barros, H. L. C. *Inorg. Chem.* **1978**, *17*, 297.
7. (a) Park, Y. K.; Kim, G. S.; Song, G. O. *Bull, Korean Chem. Soc.* **1995**, *16*, 310. (b) Pou, S. *et al. Anal. Biochem.* **1994**, *217*, 76.
8. (a) Maillard, B.; Forest, D.; Ingold, K. V. *J. Am. Chem. Soc.* **1976**, *98*, 6355. (b) Park, Y. K.; Kim, S. J. *Bull. Korean Chem. Soc.* **1990**, *11*, 109.

Characterization by Solid-State ^{51}V NMRand X-ray Diffraction of Vanadium Oxide Supported on ZrO_2

Jong Rack Sohn*, Man Young Park, and Young Il Pae

**Department of Industrial Chemistry, Engineering College, Kyungpook National University, Taegu 702-701, Korea*

Department of Chemistry, University of Ulsan, Ulsan 680-749, Korea

Received December 26, 1995

Vanadium oxide-zirconia catalysts were prepared by dry impregnation of powdered $Zr(OH)_4$ with aqueous solution of NH_4VO_3. The characterization of prepared catalysts was performed using ^{51}V solid state NMR, XRD, and DSC. The addition of vanadium oxide up to 9 mol% to zirconia shifted the phase transitions of ZrO_2 from amorphous to tetragonal toward higher temperatures due to the interaction between vanadium oxide and zirconia. On the basis of results of XRD and DSC, it is concluded that the content of V_2O_5 monolayer covering most of the available zirconia was 9 mol%. The crystalline V_2O_5 was observed only with the samples containing V_2O_5 content exceeding the formation of complete monolayer (9 mol%) on the surface of ZrO_2.

Introduction

Catalysts based on vanadia supported on various oxides are used in a variety of industrial chemical process. Vanadium oxide catalysts in combination with various promoters are widely used for several reactions including oxidation of hydrocarbons,[1,2] ammoxidation of aromatics and methylaromatics,[3] and selective catalytic reduction of NO_X by NH_3.[4] These systems have also been found to be effective catalysts for the oxidation of methanol to methylformate.[5,6] Much research has been done to understand the nature of active sites, the surface structure of catalysts as well as the role played by the promoter of the supported catalysts, using infrared (IR), X-ray diffraction (XRD), electron spin resonance (E.S.R.) and Raman spectroscopy.[6~9] So far, silica, titania and alumina[10~13] have been commonly employed as the vanadium oxide supports, and comparatively very few works have been reported for zirconia as the support for vanadium oxide.[14~16]

It is well known that the dispersion and the structural features of supported species can strongly depend on the

*To whom all correspondence should be addressed.